DIELECTROPHORETIC CELL SORTING VIA SLIDING CELLS ON 3D SILICON MICROELECTRODES

Xiaoxing Xing[1], Ming L. Chau[1], Kamyar A. Roshan[2], and Levent Yobas[1]
[1] The Hong Kong University of Science and Technology, Hong Kong, P. R. of CHINA
[2] Sharif University of Technology, Tehran, IRAN

ABSTRACT

This work presents an innovative design for a flow-through dielectrophoretic cell sorting based on silicon bulk microelectrodes featuring sidewall undercuts. The microelectrodes are configured into an interdigitated array with digits extending across the flow chamber at an oblique angle against the flow stream. Target cells under dielectrophoretic forces and hydrodynamic drag can slide along the digits to a dedicated outlet. The design has been showcased for continuous-flow sorting of viable and non-viable mammalian cells, achieving a throughput of 16,600 cells/min, an order of magnitude higher than those reported for existing continuous-flow cell sorting designs using thin-film or volumetric microelectrodes.

INTRODUCTION

An essential step in many biomedical applications from food pathogen monitoring to drug discovery and cancer diagnostics is effective separation of a target cell population from a heterogeneous mixture [1]. Practical techniques such as fluorescence or magnetic activated cell sorters target specific cell-membrane-surface ligands and thus require foreign labels. Moreover, such techniques rely on bulky expensive instruments. Lab-on-a-chip (LOC) or microfluidic devices have advanced the field of cell sorting through miniaturization and integration. Numerous microfluidic cell sorters have emerged discriminating cells based on their unique features such as affinity, size, and density in addition to their dielectric, magnetic and acoustic properties [2]. Dielectrophoresis (DEP) activated cell sorting (DACS) has drawn extensive attention owing to its label-free implementation that relies on dielectric phenotypes of cells. DACS has been applied to the separation of various cell types, such as tumor cells from blood cells [3], stem cells from their differentiated progenies [4], infected red blood cells from those healthy ones [2], and viable fungi from non-viable fungi [5].

DEP refers to the motion of a polarizable particle (e.g. a biological cell) in suspension in response to a non-uniform electric field externally applied and acting on the induced dipole moment of the particle [6]. Based on the dielectric contrast between the cell and surrounding medium, the DEP force can be either attractive (positive DEP, pDEP) or repulsive (negative DEP, nDEP) in reference to field maxima. Conventional DACS typically operates in batch mode with successive loading and elution steps [1]. During loading, target cells are trapped under pDEP while non-target cells being removed under nDEP or weak pDEP. During subsequent elution, target cells being trapped are released and retrieved by turning off the voltage. Such batch-mode operation, however, is tedious and limits the sample throughput. Moreover, prolonged trapping and exposure of cells to electric field maxima compromises the cell viability.

Separation of cells in continuous-flow mode is more attractive than in batch mode because it brings operation simplicity and increases throughput. Continuous-flow cell sorting can be achieved by deflecting target cells under a combined action of DEP and hydrodynamic drag. Target cells travelling over thin-film surface electrodes that are obliquely placed across the flow chamber bottom get deflected under DEP and directed to an adjacent sheath flow [4]. A major drawback in such design, however, is that the deflection of cells becomes ineffective as cells get distanced from the chamber bottom. Thin-film electrodes placed on both the chamber top as well as bottom address this issue to some extent, and yet demand careful assembly with precision alignment [3]. Alternatively, researchers have come up with three-dimensional (3D) volumetric microelectrodes, which extend more effective electric field profile throughout the entire channel depth. Sidewall electrodes made of metal posts, for instance, confine cells laterally into specific streams under nDEP [7]. However, fabrication of such electrodes involves gold electroplating which is expensive and time consuming. In addition to metals, other conducting materials such as heavily doped silicon, pyrolysed photoresist, or Ag-doped polymer have all been explored for the construction of effective bulk microelectrodes [5]. Nevertheless, all these designs with linear sidewalls exhibit a quasi-2D profile and fall short of exerting an effective force field along the chamber depth.

We previously showed bulk microelectrodes in doped silicon featuring a unique profile (sidewall undercuts) and thus capable of inducing a highly efficient DEP force field that segregates cells into distinct layers along the channel depth [8]. We first used these bulk microelectrodes in the construction of a silicon interdigitated array (IDA) with built-in lateral pores along the digits allowing streams of cells to run thorough without interrupting the electrical continuity. We applied this design for the enumeration of cancer cells from lymphocytes at a high cell-loading density [9]. However, the design showed a capacity of separating cells only in batch mode and failed to take full advantage of the unique electrode profile for separating cells in continuous-flow mode. Based on this electrode profile, we also introduced a relatively simple design in which a straight flow channel is flanked by a pair of bulk microelectrodes without involving electrode digits [10]. This configuration nevertheless induced electrothermal secondary flows that interfered with selective separation of cells under DEP but instead led to cell enrichment regardless of the cell type. Thus, the design has been characterized for the isolation of blood plasma.

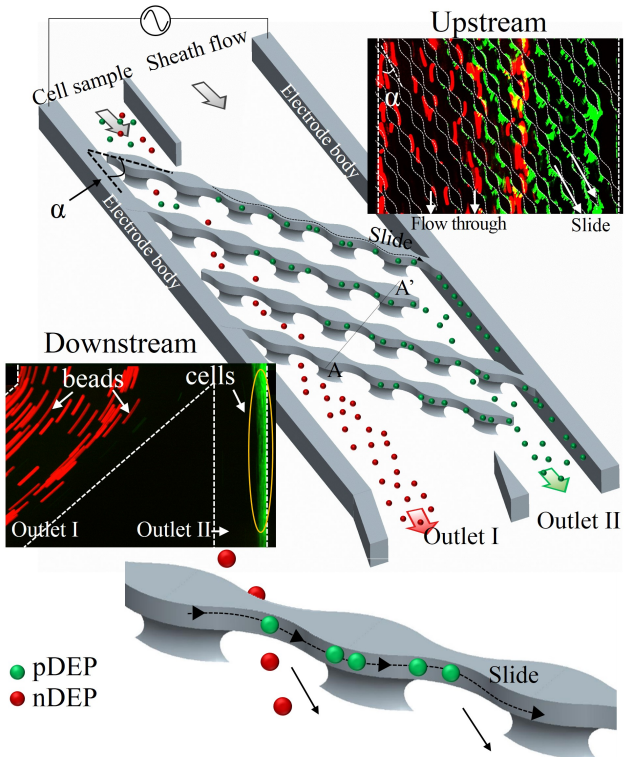

Figure 1: Illustrations describing interdigitated array of bulk microelectrodes featuring sidewall undercuts with digits aligned to the flow direction at an oblique angle α. Target cells (green) will move along the digits, sliding on the sidewalls (upper layer) to outlet II under pDEP and hydrodynamic drag. Non-target cells (red) will be repelled from the upper sidewall layer under nDEP, and, passing under the digits, flow into outlet I. Superimposed fluorescent images showing respective device sections during continuous-flow separation of cells and beads.

Here, using the unique bulk microelectrode profile, we demonstrate a microfluidic design for continuous-flow cell sorting under DEP force and hydrodynamic drag. Figure 1 schematically describes the design with inlet ports for simultaneous injection of sample and sheath buffer into a flow chamber equipped with silicon IDA microelectrodes that feature sidewall undercuts. The electrode digits span across the entire chamber depth and extend into the chamber at an oblique angle against the flow to facilitate the capturing and sliding of target cells. The monolithic electrode body presents a characteristic smooth-wavy layout along the digits to introduce flow paths at periodic sites. The sidewalls feature a linear profile along the upper layer and a concave profile along the lower layer (sidewall undercuts). Cells under pDEP get attracted to the upper layer of the sidewall where the electric field strength peaks, and then slide along the digits under hydrodynamic drag to the near side of the counter electrode body where they are guided to outlet II. Meanwhile, cells under nDEP get repelled to the lower layer and follow streamlines to outlet I. The superimposed fluorescent images show the continuous-flow separation of human colorectal cancer cells (HCT116) experiencing pDEP from those 10 μm polystyrene beads under nDEP.

MATERIALS AND METHODS

Microfabrication

The design was fabricated on a silicon-on-insulator (SOI) substrate with orientation (100) and conductivity 0.005 Ω-cm. Figure 2 describes the fabrication process, which was adopted from our previous work [8]. First, the electrode layout was patterned on a SiO_2 hard mask layer placed on the substrate and silicon was partially removed from exposed sites using deep reactive ion etch (DRIE). The entire structure was subsequently deposited with a thin layer of low-temperature oxide (LTO) followed by LTO removal from trench/chamber bottom using reactive ion etch (RIE). With the sidewalls masked under LTO, isotropic dry etch was applied to further remove silicon, forming flow paths (lateral pores) through the digits while structurally isolating the digits from the counter electrode. Finally, the LTO overhanging on the sidewalls was removed through wet etch, and the device was enclosed with a thin slab of polydimethylsiloxane (PDMS).

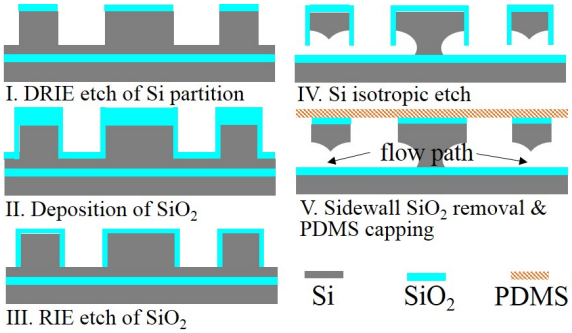

Figure 2: Illustrations describing the fabrication process on the device substrate profile after key process steps (from cutaway view AA' as delineated in Figure 1).

Experimental

Fluorescent polystyrene beads (Bangs Laboratories, diameter 10μm, Ex/Em 480/520nm) and HCT116 cells (ATCC) were used. Cells were stained by incubating with 2 μg/mL Hoechst33342 (Life Technologies, Inc.) for 20 min in the dark before washing twice with DEP buffer for 5 min at 1000 rpm. Beads were washed once using the same buffer for 2 min at 5000 rpm. Cells and beads were then mixed at a ratio 1:1 and a density 10^6 particles/mL. For the preparation of a viable/nonviable cell mixture, cells were rendered nonviable through incubation in water bath at 65°C for 15 min. Viable and nonviable cells were stained by incubating, for 20 min in darkness, with 2 and 50 μg/ml Calcein AM (Life Technologies, Inc.) and propidium iodide (PI, Sigma-Aldrich), respectively. Stained cells were washed twice using DEP buffer at 1000 rpm for 5 min and mixed at an equal density 10^6 cells/ml. To minimize cell adhesion, the chip was coated with 5% bovine serum albumin (BSA) in DEP buffer for 30 min followed by priming with the same buffer. Cells were cultured in a 5% CO_2 incubator at 37 °C with Dulbecco's Modified Eagle Medium (DMEM) supplied with 10% fetal bovine serum (FBS) and 1% penicillin. Upon harvesting, cells were washed with phosphate buffered saline (PBS) solution, trypsinized, and then suspended in fresh culture medium. DEP buffer contained 300 mM D-Mannitol in PBS with conductivity tuned to 100 μS/cm.

The sample solution and sheath buffer (DEP buffer) were delivered through syringe pumps (Harvard Apparatus). For device activation, a sine-wave voltage modulated with a square-wave at 90% duty cycle, of which each waveform was supplied by a function generator (DG1020, RIGOL), was delivered through a power amplifier (AL-50HFA, Amp-Line Corp.) and a transformer. The signal was monitored on an oscilloscope (Tektronix TDS 2012C). The images were acquired by an epi-fluorescence microscope (ECLIPSE FN1, Nikon) equipped with a colored CCD (RT3 Mono, SPOT).

RESULTS AND DISCUSSION

Fabrication results

Figure 3 depicts a representative device section captured through scanning electron microscopy (SEM). In this particular design, the digits extend at an oblique angle 7°. We have also fabricated designs with a characteristic angle 16° and 26° to evaluate their impact on cell sliding. Cells slide along the digits on the upper sidewall layer that is 15 µm thick and extends continuously. The digits feature undercuts (the concave sidewall layer) and project a characteristic wavy outline to give way to flow paths (lateral pores) underneath formed during isotropic etch. Fabrication of this monolithic structure requires only single-mask process and the lateral pores can be easily tuned by adjusting the isotropic etch time.

Cell sliding

The characteristic angle is a critical design parameter. Too small angles have hydrodynamic drag dominate over pDEP force causing cells to escape whereas too large angles have the opposite effect trapping cells on the digits under dominant pDEP forces. Here we define the sliding failure rate as the percent fraction of cells that escape into outlet I with reference to total injected cells. Figure 4 displays a bar chart indicating the sliding failure rate for the designs (angle 7°, 16°, and 26°) at sample flow rate 8.3 and 25 µL/min. We fixed the sheath flow at 5 µL/min and the activation voltage at 10 V_p and 400kHz sine wave that was modulated by 1 V_p and 1 Hz square wave with a duty cycle 90% (0.9 s on and 0.1 s off). At this activation frequency and a buffer conductivity 100 µS/cm, HCT116 cells experienced strong pDEP. Therefore, cells were levitated and attracted to the upper sidewall layer of each digit, which served as a 'track' for sliding cells. The voltage amplitude was judiciously chosen to allow cells to slide along the digits under flow rates applied within the tested range. At a sample flow rate 8.3 µL/min, all three designs exhibited a fairly low failure rate (<3%) with very few cell escapes, whereas only the design with 26° achieved a comparatively low average failure rate (~10%) at a sample flow rate 25 µL/min. This suggests that DEP trapping force acting on cells under the applied electric field strength was unable to overcome fluidic drag at the increased flow rate, and failed to retain cells sliding on tracks along the electrode digits. As expected, the design featuring a small angle exhibited a relatively high failure rate. This was due to that the fluidic drag projected along electrode digits increased with a reduced angle between digits and the main flow direction.

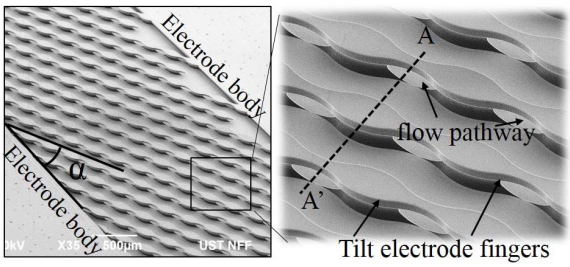

Figure 3: SEM images of a representative device section.

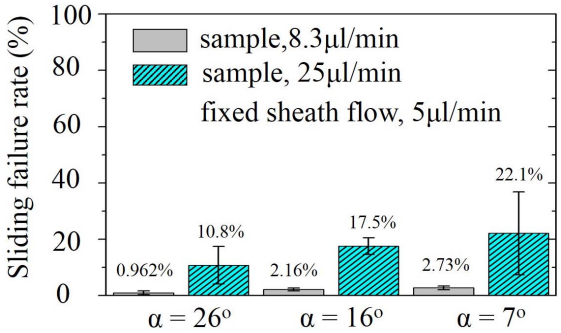

Figure 4: Sliding failure rate (those escaped to outlet I) in reference to angle α and sample injection rate (legend). Activation: 10 V_p at 400 kHz.

Viable/nonviable cell separation

We evaluated next continuous-flow sorting of viable and nonviable HCT116 cells. Viable and nonviable cells can be distinguished based on their distinct dielectric properties as validated in our previous work [10]. Cells with intact plasma membrane preserve the cytoplasm conductivity in relation to the surrounding buffer, which was kept at a relatively low conductivity (100 µS/cm). Thus, viable cells typically show strong pDEP response. Conversely, cells with breached plasma membrane become permeable to ions, losing the existing dielectric contrast between the cytoplasm and surrounding buffer. In return, nonviable cells exhibit a fairly weak DEP response.

The cell mixture and the sheath flow were injected at a rate 8.3 µL/min and 5 µL/min, respectively. Without the voltage activation, viable (green) and nonviable (red) cells stayed within their course passing through the digits and exiting the device through outlet I as depicted in Figure 5. Upon activation (10V_p at 400kHz), however, nonviable cells came under only weak DEP and continued to remain on course until exiting through outlet I. On the contrary, a major fraction of viable cells became drawn to the electrode digits under strong pDEP and continued to travel downstream by sliding along the digits until they reached the digit ends. Once at the digit ends, these cells either became released during the activation off cycle or passed onto the counter electrode body where they continued to slide down. In this way, all viable cells that successfully migrated across the flow chamber entered into outlet II. We also noticed that viable cells as they slide along a digit preferred the sidewall facing downstream suggesting an excessive and persistent fluidic drag that overtook pDEP on the sidewall facing upstream.

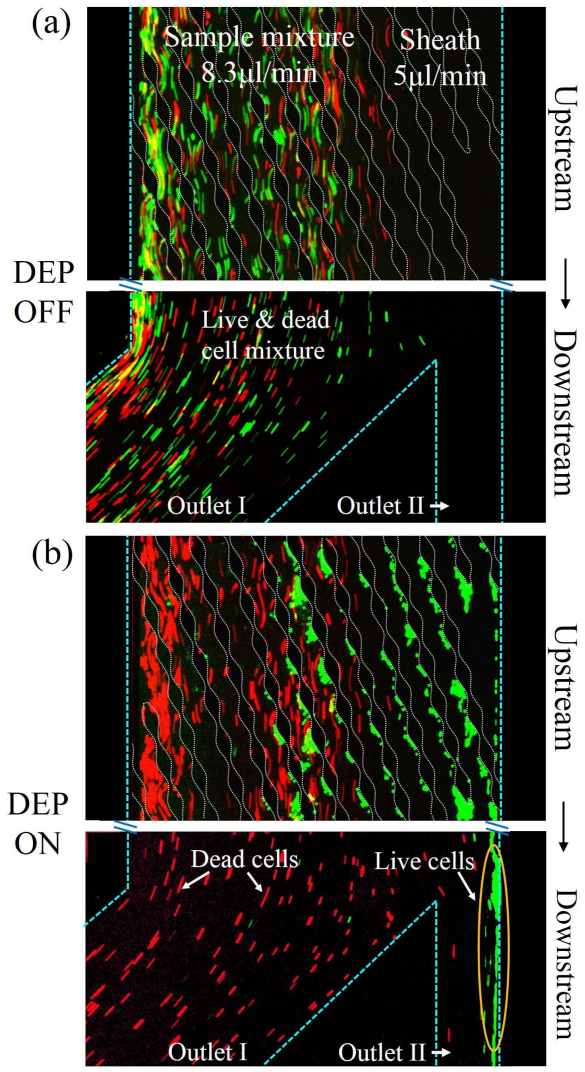

Figure 5: Continuous-flow separation of viable (green) and nonviable (red) cells in superimposed fluorescent images: (a) before and (b) after voltage activation using a sine wave (10 V_p at 400 kHz) modulated by a square wave (1 V_p at 1 Hz and 90% duty cycle) Sample and sheath flow: 8.3 and 5 µL/min, respectively.

CONCLUSION

We have introduced a novel microfluidic device for continuous-flow cell sorting via sliding cells on silicon bulk microelectrodes by effectively coupling DEP force and hydrodynamic drag. Fabricated through a single-mask process, the microelectrodes feature sidewall undercuts and the corresponding DEP force field segregate cells into distinct layers along the channel depth based on their phenotype. We have also evaluated the failure rate of sliding cells against the sample flow rate and the characteristic angle followed by the electrode digits extending into the chamber. We have further shown the device capacity for continuous-flow sorting of viable and nonviable cells at a throughput ~16,600 cells/min, an order of magnitude higher than those delivered by existing continuous-flow sorters either using planar surface electrodes [4] or volumetric electrodes [5]. The excellent performance delivered in sorting cells makes the device a promising candidate to serve as a front-end module in an integrated LOC microsystem for biomedical and clinical applications.

ACKNOWLEDGEMENTS

This work was financially supported by the Research Grant Council of Hong Kong under Grant 16211714.

REFERENCES

[1] I. Doh and Y. H. Cho, "A continuous cell separation chip using hydrodynamic dielectrophoresis (DEP) process," *Sens. Actuator A-Phys.*, vol. 121, pp. 59-65, May 2005.

[2] T. Braschler, N. Demierre, E. Nascimento, T. Silva, A. G. Oliva, and P. Renaud, "Continuous separation of cells by balanced dielectrophoretic forces at multiple frequencies," *Lab Chip*, vol. 8, pp. 280-286, 2008.

[3] J. Park, B. Kim, S. K. Choi, S. Hong, S. H. Lee, and K. I. Lee, "An efficient cell separation system using 3D-asymmetric microelectrodes," *Lab Chip*, vol. 5, pp. 1264-1270, 2005.

[4] H. J. Song, J. M. Rosano, Y. Wang, C. J. Garson, B. Prabhakarpandian, K. Pant, et al., "Continuous-flow sorting of stem cells and differentiation products based on dielectrophoresis," *Lab Chip*, vol. 15, pp. 1320-1328, 2015.

[5] N. Lewpiriyawong, K. Kandaswamy, C. Yang, V. Ivanov, and R. Stocker, "Microfluidic Characterization and Continuous Separation of Cells and Particles Using Conducting Poly(dimethyl siloxane) Electrode Induced Alternating Current-Dielectrophoresis," ," *Anal. Chem.*, vol. 83, pp. 9579-9585, Dec 2011.

[6] T. B. Jones, *Electromechanics of Particles*: CAMBRIDGE University Press, 1995.

[7] L. Wang, L. A. Flanagan, N. L. Jeon, E. Monuki, and A. P. Lee, "Dielectrophoresis switching with vertical sidewall electrodes for microfluidic flow cytometry," *Lab Chip*, vol. 7, pp. 1114-1120, 2007.

[8] X. Xing, R. Y. C. Poon, C. S. C. Wong, and L. Yobas, "Label-free enumeration of colorectal cancer cells from lymphocytes performed at a high cell-loading density by using interdigitated ring-array microelectrodes," *Biosens. Bioelectron.*, vol. 61, pp. 434-442, Nov 15 2014.

[9] X. Xing, M. He, H. Qiu, and L. Yobas, "Continuous-Flow Electrokinetic-Assisted Plasmapheresis by Using Three-Dimensional Microelectrodes Featuring Sidewall Undercuts," *Anal. Chem.*, vol. 88, pp. 5197-5204, May 2016.

[10] X. Xing and L. Yobas, "Dielectrophoretic isolation of cells using 3D microelectrodes featuring castellated blocks," *Analyst*, vol. 140, pp. 3397-3405, 2015.

CONTACT

*L. Yobas, tel: +852-23587068; eelyobas@ust.hk